# Advanced techniques for the study of shrinkage-induced cracking of concrete with recycled aggregates at early age

A.Z. Bendimerad, B. Delsaute, Emmanuel Rozière, S. Staquet, Ahmed Loukili

# Advanced techniques for the study of shrinkage-induced cracking of concrete with recycled aggregates at early age

A.Z. Bendimerad[1], B. Delsaute[2], E. Rozière[1], S. Staquet[2], A. Loukili[1]

(1) Ecole Centrale de Nantes, Civil engineering and Mechanics research Institute (GeM) – UMR CNRS 6183, 1 rue de la Noé, 44321 Nantes cedex 3, France.

(2) Service BATir, Université Libre de Bruxelles, 87 Avenue A. Buyl, 1050 Bruxelles, Belgium.

## Abstract

The present work analyses the impact of the substitution of natural coarse gravel and sand by recycled gravel and sand on the concrete behavior under free and restrained condition since setting. The methodology presented in this paper associates a Temperature Stress Testing Machine (TSTM) with free shrinkage tests and other experimental advanced techniques, such as direct tensile testing and the monitoring of elastic properties using repeated loading testing. It is observed that the cracking sensitivity decreased with recycled concrete content in spite of lower tensile strength. This is due to the major influence of relaxation, but also damage and coupling effects. These phenomena contributed to a decrease of the stresses with different magnitude and kinetics. For concretes with recycled gravels, the major stress reduction was attributed to relaxation. The reduction of elastic modulus due to damage appeared from the first 24 hours while creep seemed to develop later, as tensile stress to strength ratio became higher. Concrete with recycled sand had a different behavior with earlier creep development and lower damage.

Keywords: Shrinkage, relaxation, cracking, recycled concrete, early-age, restrained shrinkage

## 1. Introduction

The use of construction and demolition waste as an alternative source of aggregates for the production of new concrete has become more common for the last decade. In many urban areas, a critical shortage of good quality natural aggregates is detected. At the same time old buildings and structures are demolished due to their obsolescence, generating waste materials in these same areas. In France, 300 million tons of building wastes are produced each year [1]; only a part is used for new constructions, mainly for road works. The use of recycled concrete aggregates is promoted as it is expected to reduce $CO_2$ emission, energy consumption and the use of natural raw materials. However materials used for structural concrete have to comply with the requirements from standards and building codes in terms of composition and mechanical properties [2]. These requirements are meant to provide users with safety and serviceability of concrete structures for their whole service life. In this framework, in France, the National Projects RECYBETON [1] and ECOREB [3] were carried out in order to develop recommendations for the use of recycled aggregates in building materials.

The influence of aggregates on short and long-term behavior of concrete is significant[4,5]. Particle size distribution, shape, nature, porosity (measured as water absorption), and initial water saturation affects workability, plastic stage, setting and hardening, strength, shrinkage, creep, thus durability [6]. Many studies regarding recycled concrete (RC) aggregates can be found in the literature. These studies mainly focus on the influence of RC aggregates proportion on the properties of hardened concrete [7–9]. It was mainly observed that the replacement of natural aggregates by recycled ones induces a decrease of the density, freezing and thawing resistance and mechanical performances and an increase of the drying shrinkage [10]. However, at early age, the volume change of cement-based materials is significant and is partially or fully restrained. When shrinkage is restrained, tensile stresses are induced and

cracking is likely to occur. To ensure the durability of the concrete structure, it is needed to prevent or to limit this risk. As a consequence, the development of the deformation induced by hydration (thermal and autogenous strain) and desiccation (drying shrinkage) should be experimentally defined as the mechanical properties (compressive and tensile strength, elastic modulus and creep/relaxation) [11]. However, only few studies have been performed on these early age properties of recycled concrete (see e.g. [12,13]). It is shown that using RC aggregates generally resulted in delayed cracking and lower stresses [14,15]. The evolution of the properties involved in cracking sensitivity is actually coupled when shrinkage is restrained. For example creep/relaxation mitigates the stress development and the stress level influences creep. RC aggregates are porous thus they can absorb or release water. The absorption coefficient depends on the fraction (fine or coarse) and the origin of recycled aggregates. During the hydration process, recycled aggregate can be considered as a water tank for the cement paste and thus plays the role of an internal curing agent [16]. This phenomenon reduces and/or delays the decrease of the internal relative humidity of the cement paste [17,18]. The internal curing effect was firstly observed on concrete composed of porous [6] or lightweight aggregate in sealed and drying conditions [19–21] but also on crushed returned concrete aggregates and recycled aggregates [22,23]. The release of water from RC aggregates has been highlighted by Salgues et al. [24]. They directly monitored the water saturation of aggregates from mixing time to 2 hours and showed that the actual absorption of RG was higher in cement paste then aggregates started to release water from 0.5 hours in drying conditions but not in sealed conditions. The release of aggregates water probably occurred later. As the pores of hydrating cement paste become progressively finer than the pores of porous aggregates, these release water, according to Kelvin-Laplace equation [20]. In consequence, the substitution of natural aggregates by recycled ones decreases the self-desiccation and the desiccation of concrete at early age.

Research related to the influence of recycled concrete on plastic shrinkage and the associated cracking sensitivity at early age is rather scarce. The ability of RC aggregates to provide internal curing has been showed by several studies [22,25] but the same authors reported an increase in drying shrinkage and plastic shrinkage, respectively. However the consequences of these evolutions on cracking sensitivity have not been investigated yet. The authors already showed the influence of RC on the cracking sensitivity at very early age [26], i.e. before cracking, when fresh concrete is subjected to differential settlements. The shrinkage-to-weight loss ratio and cracking risk were mainly influenced by the total water-to-binder ratio, where total water includes the water added and the water used to pre-saturate the aggregates. Another critical period is setting and early hardening stage, as this period corresponds to the minimum of tensile strain capacity [27,28]. If the tensile strength is lower than the stress caused by restrained movement, shrinkage cracking occurs [29,30]. Active restrained shrinkage test rigs have been developed to investigate these phenomena [30–32] but only few studies deal with the influence of porous aggregates at early age [33] and none with RC aggregates. Finally, the authors have also shown that, under sealed condition, recycled sand and gravels reduces the risk of cracking of concrete structure, which highlights the interest of these components for mass concrete [34]. However, further experimental and numerical investigations are still required to understand the impact of recycled aggregate on the early age cracking sensitivity of recycled concrete [14,15,35,36].

The study presented in this paper focuses on plastic shrinkage induced cracking of concrete with recycled sand and gravels at early age. The experimental part is based on active restrained shrinkage tests performed with the temperature-stress testing machine (TSTM) at ULB in Brussels, Belgium. This system has been developed in the Laboratory of Civil Engineering of ULB since 2006 [37,38] and the system was significantly updated for this study in drying conditions. This test was associated to free shrinkage tests and other

experimental advanced techniques, such as direct tensile testing and the monitoring of elastic properties using repeated loading testing in order to characterize the properties of recycled concrete since very early age under free condition. Several phenomena are actually coupled in the conditions of restrained shrinkage thus it is necessary to monitor the evolution of the same properties in unrestrained conditions to estimate the coupling effects and understand the influence of the different properties on the evolution of cracking sensitivity. In the following sections the experimental program is first presented. Four concrete mixtures were studied, namely: natural aggregates (NA) concrete, two concrete mixtures with 30% and 100% of coarse RC aggregates, and one mixture with RC sand. The TSTM and the experimental procedures corresponding to the other advanced testing procedures are then described. The results are analysed and discussed, first free shrinkage then restrained shrinkage. The evolution of stresses and the different properties are analysed and finally a methodology is described to quantify the contributions of the main phenomena in the evolution of the cracking sensitivity and to understand the influence of the proportion and type of RC aggregates.

## 2. Methodology

### 2.1 Experimental program, materials and mixtures

The experimental program focuses on the replacement of natural aggregates by recycled concrete (RC) aggregates. Four concrete mixtures are studied in the framework of the French National Project RECYBETON. Concretes are named “XRSYRG” where X and Y are the percentage of replacement of natural sand and gravels by recycled ones in volume respectively. Recycled sand corresponds to 0 – 30% of the sand volume fraction and recycled gravels correspond to 0 – 30 – 100% of the gravel volume fraction. A moderate substitution ratio of 25 to 30% corresponds to most of recommendations [39,40]. However, a full

replacement allows a better understanding of the phenomena involved in shrinkage-induced cracking. Moreover, in a recent review, Verian et al. [40] concluded that higher proportions (up to 100%) can be used if the mix design, batching methodology, and the moisture condition of the aggregates are properly handled. For instance, Arezoumandi et al. [41] showed that beams with 100% recycled concrete aggregate had comparable ultimate flexural strength. Adams et al. [36] found that the use of RCA up to 100% significantly reduced the cracking risk of concrete. RC sand and coarse aggregates were initially at the saturated surface dried condition (SSD) state. The water content of cement paste and the properties of concrete actually depend on the initial water saturation of porous aggregates [6] and RC aggregates [42]. The properties of RC aggregates are detailed in Table 1.

Table 1 - Properties of natural and recycled aggregates

| | **Natural aggregates** | | | **Recycled concrete aggregates** | | |
|---|---|---|---|---|---|---|
| | **Sand 0/4mm** | **Gravel 4/10mm** | **Gravel 6.3/20mm** | **Sand 0/4mm** | **Gravel 4/10mm** | **Gravel 10/20mm** |
| **Mineralogy** | Silico-calcareous | Dense limestone | Dense limestone | Demolition waste | Demolition waste | Demolition waste |
| **Water absorption $WA_{24}$ (%)** | 1.2 | 0.56 | 0.53 | 10.7 | 5.3 | 4.9 |
| **Density ($g/cm^3$)** | 2.6 | 2.73 | 2.73 | 2.10 | 2.34 | 2.32 |

Natural sand from Sandrancourt, France was used, and natural coarse aggregates were crushed dark limestone from Givet, France. RC aggregates were obtained by crushing unknown waste concrete from Paris region, France. They can be considered as good quality RC aggregates according to standard NF EN 206/CN [43,44]. Their coefficient of water absorption at 24 hours $WA_{24}$ was determined using pycnometer and hydrostatic weighing and both methods gave consistent results [45]. Limestone filler from Orgon and Portland cement

CEM II/A-L 42.5 N from Rochefort, France were also used. Their main properties and composition are given in Table 2. All the materials were provided by French National Project RECYBETON. This project aimed at investigating the use of RC aggregates for structural concrete.

Table 2. Properties of cement and limestone filler

| | **Composition (%)** | | **Blaine fineness ($cm^2/g$)** | **Standard compressive strength (MPa)** | **Density ($g/cm^3$)** |
|---|---|---|---|---|---|
| | **Clinker** | **Limestone** | | | |
| **Limestone filler** | - | 99 | 4600 | - | 2.7 |
| **Cement** | 87 | 11 | 3700 | 53 | 3.09 |
| | **Compound composition of clinker (%)** | | | | **$Na_2O$eq (%)** |
| | **$C_3S$** | **$C_2S$** | **$C_3A$** | **$C_4AF$** | |
| | 61 | - | 7.9 | 12 | 0.59 |

The four studied concrete mixtures (

Table 3) were designed to reach the minimal strength of C25 class and the slump of S4 class [46,47]. The superplasticizer (SP) was a high-range water-reducing admixture based on polycarboxylate ether (PCE). The SP content was adjusted to reach the slump. The effective water content $W_{eff}$ is the difference between the total water content $W_{tot}$ and the water absorbed by aggregates $W_{abs}$ according to their nominal absorption $WA_{24}$ (equation 1). The equivalent binder content $B_{eq}$ is calculated according the definition of Standard NF EN 206 [43], with a coefficient of activity $k = 0.25$ for limestone filler (equation 2). The $W_{eff} / B_{eq}$ ratio was kept constant but the paste volume, thus water and cement contents, was slightly increased for mixtures with RC aggregates to reach the target slump.

159 $$W_{tot} = W_{eff} + W_{abs} \quad \textbf{(1)}$$

160 $$B_{eq} = C + k.L \quad \textbf{(2)}$$

161

162 Table 3. Studied concrete mixtures

| | **0RS-0RG** | **30RS-0RG** | **0RS-30RG** | **0RS-100RG** |
|---|---|---|---|---|
| **NG 6,3/20** (kg/m$^3$) | 820 | 829 | 462 | - |
| **RG 10/20** (kg/m$^3$) | - | - | 296 | 701 |
| **NG 4/10** (kg/m$^3$) | 267 | 190 | 228 | - |
| **RG 4/10** (kg/m$^3$) | - | - | - | 163 |
| **NS 0/4** (kg/m$^3$) | 780 | 549 | 813 | 806 |
| **RS 0/4** (kg/m$^3$) | - | 235 | - | - |
| **Cement, *C*** (kg/m$^3$) | 270 | 276 | 276 | 282 |
| **Limestone, *L*** (kg/m$^3$) | 45 | 31 | 31 | 31 |
| **Superplasticizer SP** (kg/m$^3$) | 0.747 | 0.798 | 0.861 | 0.798 |
| $W_{eff}$ (L/m$^3$) | 180 | 185 | 185 | 189 |
| $W_{tot}$ (L/m$^3$) | 194.6 | 221.4 | 212.3 | 241.0 |
| $W_{eff}/B_{eq}$ | 0.64 | 0.65 | 0.65 | 0.65 |
| **Volume of paste (l/m$^3$)** | 285 | 287 | 287 | 293 |
| **Gravel/Sand** | 1.39 | 1.30 | 1.21 | 1.07 |
| **Slump (mm)** | 195 | 204 | 193 | 195 |
| **Compressive strength, $f_{c28\ d.}$** | 31.4 | 29.0 | 28.5 | 27.6 |

163

164

## 2.2 Testing procedures

### 2.2.1 Tensile strength

Tensile strength has been determined on ∅11x22 (in centimetres) cylindrical specimens using the splitting tensile test and on prismatic specimens by using direct tensile test [28]. In addition the tensile strain capacity is tested with the direct tensile test. Direct tensile testing [28] has been performed on mixtures at several ages from 7 to 24 hours (7 – 10 – 16 – 20 and 24h). For each age of loading, 2 cylindrical samples were tested to define the splitting tensile strength and one direct tensile test was performed. Data related to the repeatability of this test can be found in previous work [28]. The average difference between two strength values at the same age was 6%. The average difference between two values of tensile strain capacity was 21%. In order to obtain the evolution of the tensile strength throughout the whole time period of the TSTM tests, these values have been extrapolated using data from the splitting tensile test.

### 2.2.2 Elastic modulus

The static modulus $E_{stat}$ was assessed through repeated compression tests [48–50] on cylindrical samples. One cylindrical sample was used for each concrete mixture. A vertical testing device has been designed at ULB to monitor the elastic and basic creep properties [51]. Compressive loadings can be applied a few hours after the final setting. An electromechanical testing setup with a capacity of $\pm$ 100kN is used. The machine is fully controlled by computer (load and displacement). A cylindrical concrete specimen (97 mm in diameter and 550 mm in height) is cast inside a Polyvinyl chloride (PVC) mold. Before casting, a thermocouple is placed in the center of the mold of the dummy specimen. After casting, all specimens are stored in an air-conditioning chamber at 20°C and 90% relative humidity. Then samples are demolded, grinded on both circular end faces and covered by 2

189 self-adhesive aluminum sheets in order to keep the sample in sealed conditions. The sealing
190 has been checked by weighting the sample before and after the test. No significant weight loss
191 was observed. As samples are grinded few hours after setting, a thin layer of sieved concrete
192 (1cm) is placed on the top of the sample in order to avoid pulling out aggregates during
193 grinding. All the equipment is in an air-conditioned room. Displacements are measured with
194 an INVAR© extensometer composed by two rings spaced of 350 mm and three rods which
195 hold the 3 longitudinal displacement sensors placed at 120°. 3 lateral displacement sensors are
196 placed on the lower ring. Both rings are fixed to the specimens by means of three elastic
197 anchorages allowing the measurement of the longitudinal and lateral displacement.

198 The tests were performed from the end of setting and the load did not exceed 20% of the
199 compressive strength at each loading. The sample is loaded in compression in 10 seconds at a
200 constant stress rate then unloaded till a value of 0.014 MPa to always keep a contact between
201 the sample and the testing device. This threshold value is chosen to avoid any damage of the
202 sample in compression. The static E-modulus is determined during the repeated loading from
203 the data (measured load and displacement) between 30% and 80% of loading [48,49,52]. The
204 data provided by this testing procedure has been compared to other classical and non-
205 destructive methods [49].

206 ### 2.2.3 Temperature Stress Testing Machine (TSTM)

207 A TSTM has been developed at the civil engineering laboratory BATir at ULB (Université
208 Libre de Bruxelles) since 2006. This system allows characterizing concrete from very early-
209 age in free and restrained conditions [37,38]. It consists of a TSTM frame and a dummy mold.
210 An overview of the whole test setup is shown in Figure 1.

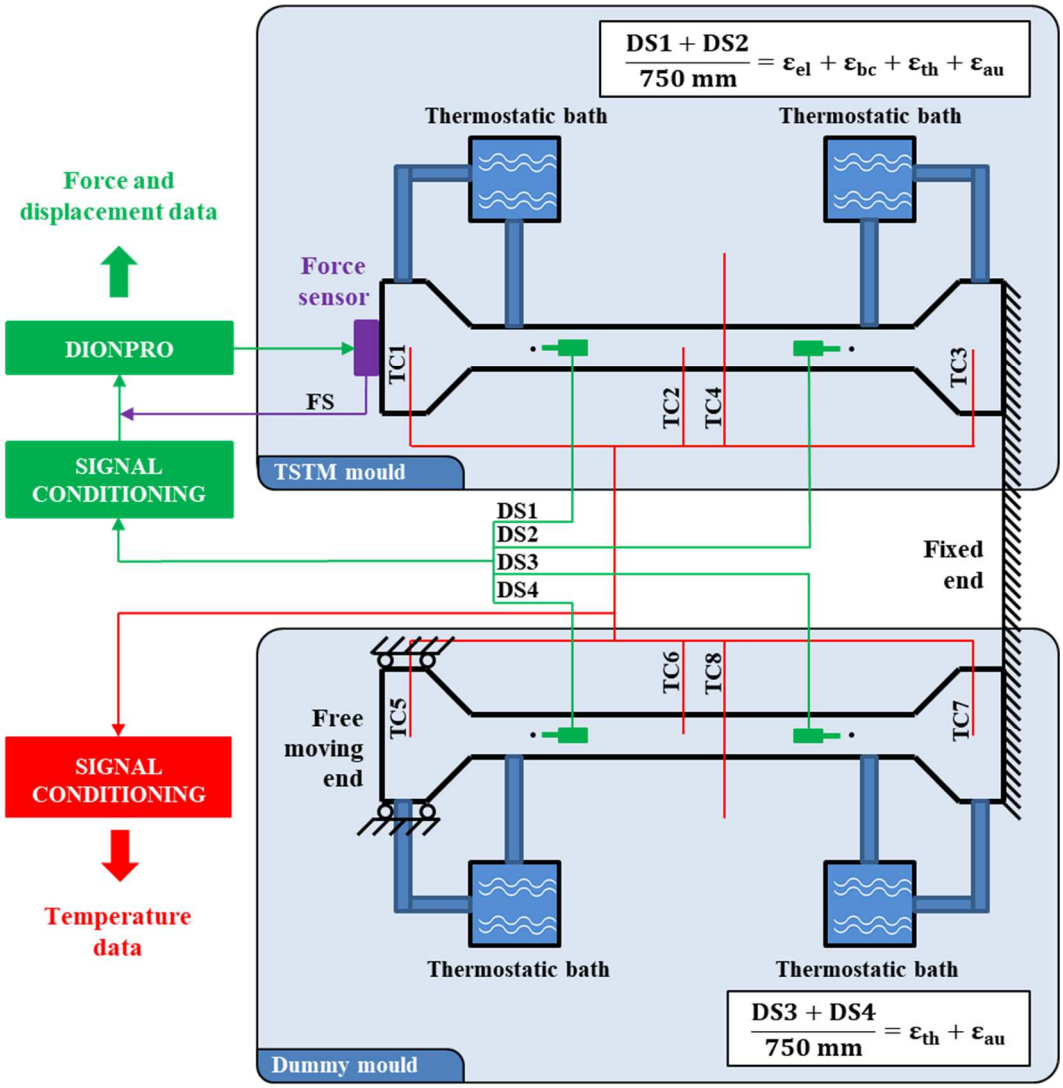


Figure 1 – Scheme of the TSTM [52]

The restrained shrinkage frame is based on a Walter+Bay ±400 kN electromechanical testing setup. The concrete specimen has a dog-bone shape with a longitudinal part of 1000 mm with a 100x100 mm² cross-section in the central part and a 300x100 mm² section at both ends (Figure 2). The dimensions allow testing concrete mixtures with a 20-mm maximum aggregate size. Concrete sample is poured in the double-walled mold connected to a temperature-control system set at 20°C for the tests presented in this paper. The test takes place in a climate room (20°C – 50%RH) and only the top face is exposed to drying after casting. Thermocouples are placed at the center and at both ends of the mold in order to monitor the evolution of the actual temperature in the sample. The displacements are

measured by sensors without contact with a resolution of 0.014 µm which are placed on invar supports. These sensors are located at mid height of the sample at a distance of 750 mm, where the stress field is assumed to be homogenous. They are fixed on steel bars externally supported by the TSTM frame (Figure 3). The TSTM allows performing restrained shrinkage test but also to assess the evolution of the creep or the elastic modulus since setting [52,53].

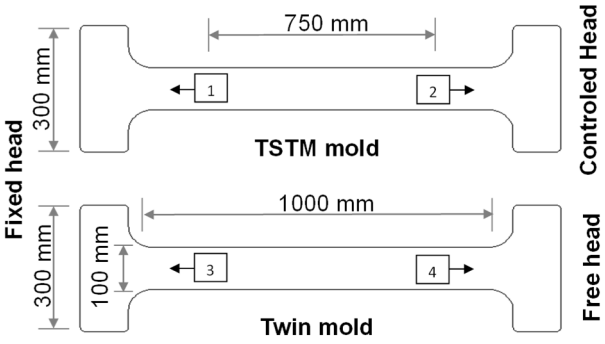


Figure 2. TSTM and twin mold with their dimensions [38].

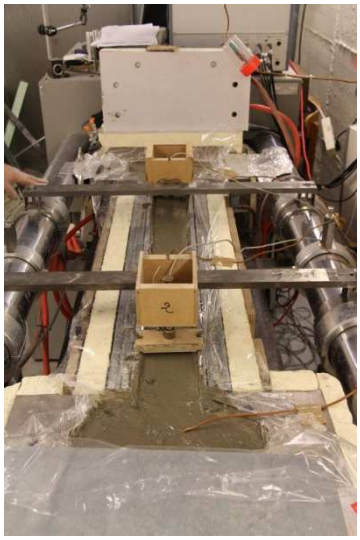

Figure 3. TSTM mold with displacement sensors and thermocouples in place (concrete 0RS-0RG).

A twin mold was built to measure the free strain. This mold has exactly the same geometry as the TSTM mold (Figure 2); the displacement of the free end is not externally controlled.

The total strain in the TSTM $\varepsilon_{TSTM}$ mold is calculated assuming that the strain components are independent, thus it corresponds to the sum of the following strains: elastic $\varepsilon_{elas}$, creep $\varepsilon_{creep}$, thermal $\varepsilon_{ther}$ and shrinkage $\varepsilon_{sh}$. This will be defined as the cumulated strain (equation 3).

$$\varepsilon_{TSTM} = \varepsilon_{elas} + \varepsilon_{creep} + \varepsilon_{ther} + \varepsilon_{sh} \quad (3)$$

The strains in the twin mold correspond to the sum of the thermal and shrinkage strains as shown by equation 4.

$$\varepsilon_{free} = \varepsilon_{ther} + \varepsilon_{sh} \quad (4)$$

Subtracting the twin mold strain from the TSTM mold strain gives the elastic and creep strain (equation 5). The simultaneous use of both molds allows the determination of creep effects.

$$\varepsilon_{TSTM} - \varepsilon_{free} = \varepsilon_{elas} + \varepsilon_{creep} \quad (5)$$

The restrained shrinkage tests started at the end of setting. At this age, concrete is stiff enough to hold the rods used for strain measurement. At this time, the strain sensors are reset and the TSTM test starts. The concrete in the TSTM mold starts shrinking freely until it reaches a strain of 6.2 µm/m (Figure 4). Then, the controlled head moves in the opposite direction in order to reset the strain. After this, the load is maintained constant; meanwhile, the concrete keeps contracting until the strain reaches the threshold value again. A new compensation cycle then begins and the test continues until cracking or when the test duration exceeds 2 weeks. The threshold strain value has been defined by considering that it must be as low as possible to be as close as possible to a full restraint situation during the whole test and at the same time high enough to compute accurately the viscoelastic properties (elastic modulus and creep strain) for each compensation cycle [54].

The cumulated strains of the TSTM mold and the free strains of the twin mold for the conventional concrete 0RS-0RG are displayed in Figure 4 and Figure 5. The thermal strains of studied concrete were around 10µm/m, thus the corrected and uncorrected strains are close.

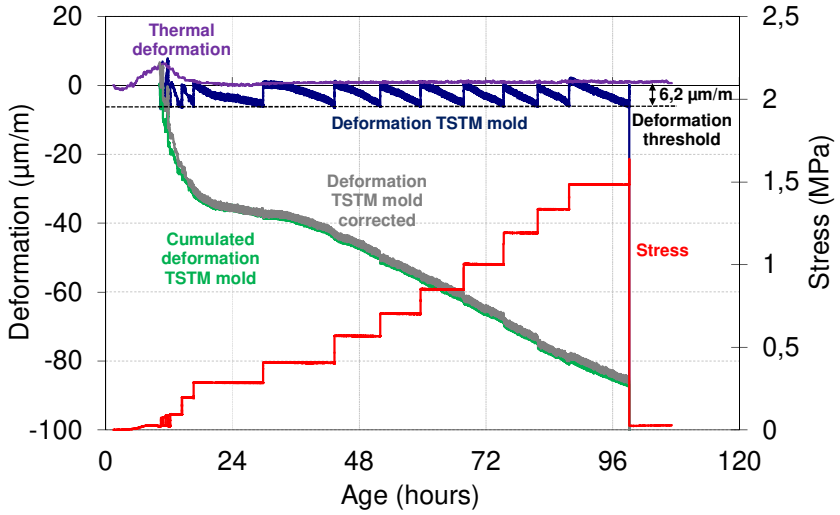


Figure 4. Strain and stress in the TSTM mold: restrained shrinkage.

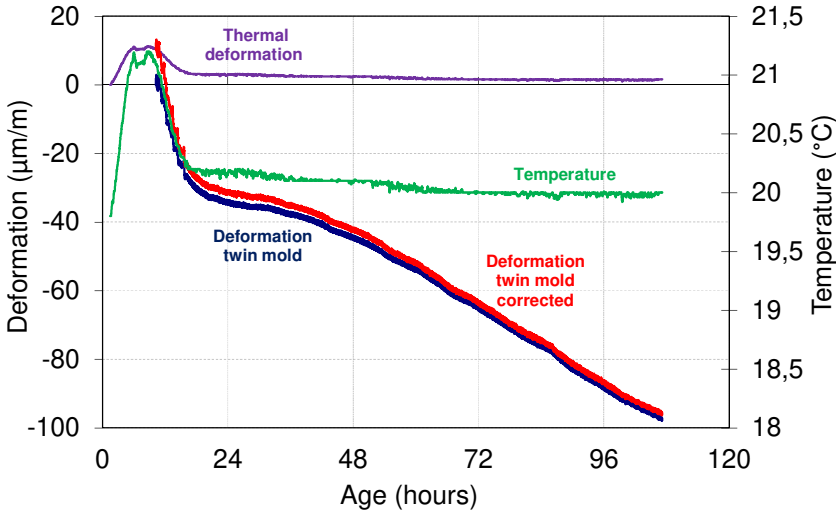


Figure 5. Strain in the twin mold: free shrinkage.

Each concrete mixture was tested once but 0RS-100RG was tested twice in order to estimate the repeatability of the system. This concrete mixture was chosen as RC aggregates are often considered to induce higher variability of concrete properties due to their heterogeneous nature. The results are plotted on Figure 6 and Figure 7. The literature data has not provided any repeatability tests for the TSTM except in the study of Klausen [55] who also showed a good repeatability of such tests in spite of their complexity. The first test lasted 12 days without cracking and the second was stopped after 7 days to save testing time for other tests. The stress development due to the restraint in the TSTM mold and the evolution of the free

261 strains in the twin mold are presented in Figure 6 and Figure 7 respectively. The repeatability
262 was considered as acceptable for the presented experimental study.

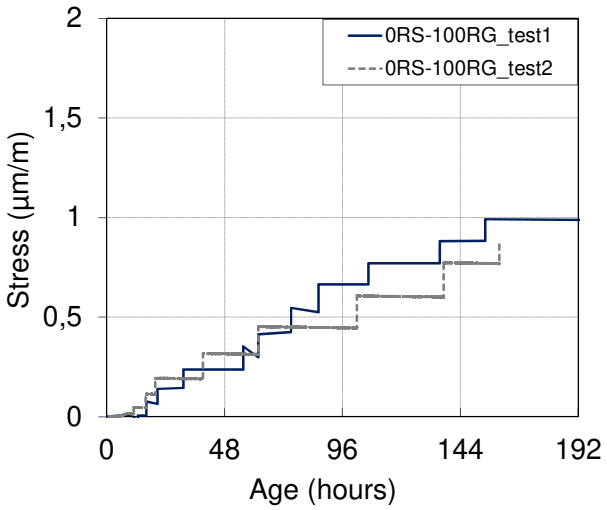


Figure 6. **Repeatability testing: evolution of stress in 100% RG concrete.**

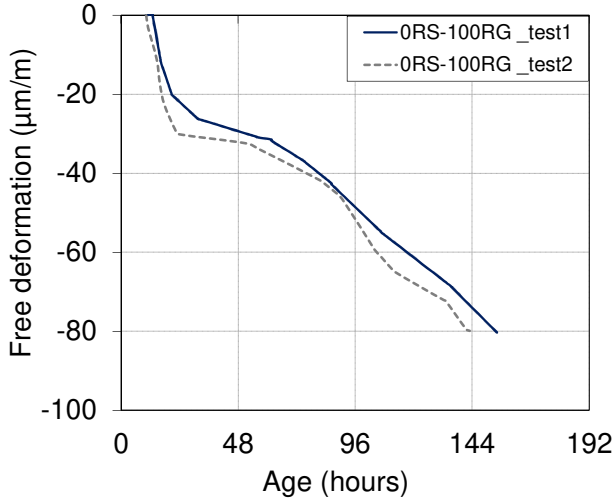


Figure 7. **Repeatability testing: free shrinkage in 100% RG concrete.**

263

264 During the TSTM test, the evolution of the applied load is measured to determine the
265 cumulated stresses in concrete. The static elastic modulus of the concrete can be determined
266 during each load cycle in the TSTM mold. Knowing the tensile stress increment and the strain
267 increment, Hooke's law can be applied to calculate the modulus $E_{TSTM}$ during the restrained
268 shrinkage test. It is calculated as shown in Figure 8 and according to equation 6, using the
269 values between 20 and 80 % of the load increment.

$$E_{TSTM}(t_i) = \frac{\Delta\sigma_i}{\Delta\varepsilon_i} \tag{6}$$

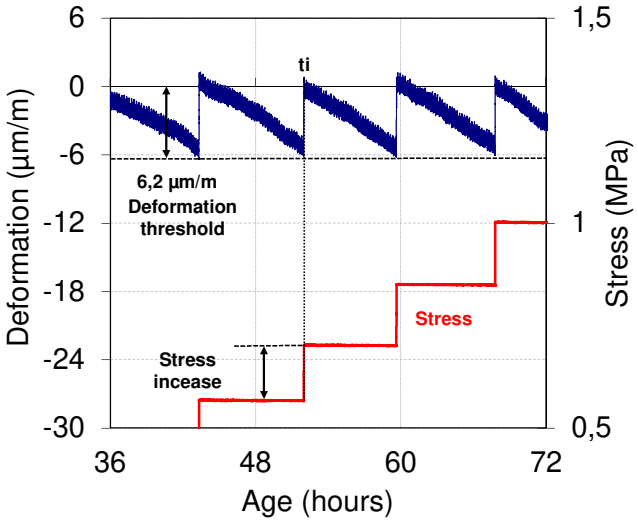


Figure 8. **Determination of elastic modulus from the TSTM tests**

## 3. Results and discussion

Shrinkage-induced cracking depends on several properties of concrete, namely: elastic modulus, free strain, creep, tensile strength, fracture energy. In this experimental study TSTM was associated to other advanced techniques in order to understand the influence of RC aggregates proportion of concrete properties and cracking potential at early-age.

### 3.1. Elastic modulus

Measurements started 4 hours after setting. The whole test duration was 1 week or more and the test was performed on one cylindrical sample. The temperature of the sample is set to 20°C. For each repeated loading, the E-modulus is calculated from the load and displacement data between 30% and 80% of loading [48,49]. Results are plotted against the age of the specimen in

Figure 9. The substitution of 30% of natural coarse aggregates by RG does not change significantly the evolution of the E-modulus whereas a substitution of 100% induces a decrease of the E-modulus by 5 GPa at an age of 1 week. The substitution of 30% of natural sand by recycled sand induces a decrease of the elastic modulus by 4 GPa at an age of 1 week. The 0RS-30RG concrete has a limited RC content (

Table 3). As RG have relatively low paste content, they do not affect much the elastic modulus of concrete for low replacement rate [14]. The 0RS-100RG concrete globally showed lower moduli. This is due to the lower modulus of RC 4/10 as they include more old cement paste than RG 10/20 [56] (

Table 3). Elastic modulus has actually been reported to decrease with paste volume [57]. The amount of old cement paste is even higher in recycled sand. This explains why a substitution of 30% of natural sand by recycled one has a similar impact to the elastic modulus than a full replacement of natural gravels by recycled ones. Similar experimental results were obtained previously by other researchers. On hardened concrete, Thomas, *et al.* [12] have shown that very small reduction of the elastic modulus takes place when the replacement of natural gravels by recycled ones is lower than 25%. For higher replacement ratio, a significant decrease of the elastic modulus was obtained. On hardening concrete, Velay-Lizancos, *et al.*[58] have observed that low substitution (<30%) of natural sand by recycled one decreases significantly the elastic modulus. Omary et al. [56] also observed a significant reduction in elastic modulus with 30% of recycled sand. This reduction was almost as high as the reduction due to full replacement of natural gravels by recycled ones, as observed here (Figure 9).

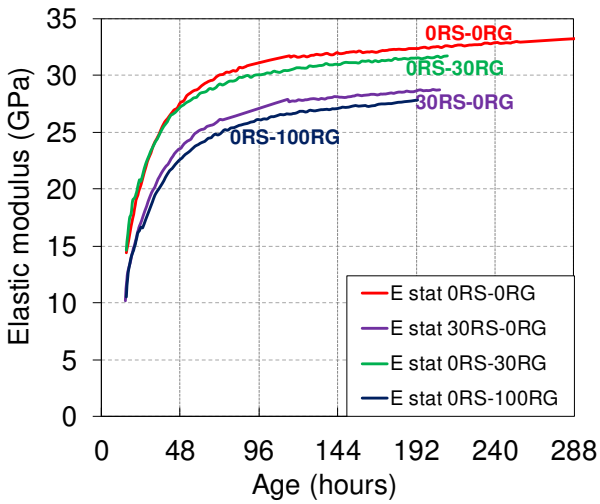


Figure 9**.** Effect of substitution rate on the elastic modulus determined from repeated loading tests.

### 3.2 Tensile strength and tensile strain capacity

Direct tensile testing has been performed at several ages from 7 to 24 hours. One sample was tested for each age at loading (7 – 10 – 16 – 20 and 24h). In order to obtain the evolution of the tensile strength throughout the whole time period of the TSTM tests, these values have been extrapolated using data from the splitting tensile test (tests performed at several ages from 16 to 300 hours as shown in Table 4), by applying the ratio of splitting tensile strength to direct tensile strength according to equation 7 derived from the theory of elasticity, with F the measured peak load [kN], D the sample diameter [cm], and L the length of the specimen [cm]. Two cylindrical samples were tested for every age at loading and the results presented correspond to the average of both samples.

$$f_{t,d} = 0.9 f_{t,sp} = 0.9 \cdot \frac{20 \cdot F}{\pi \cdot D \cdot L} \quad \textbf{(7)}$$

Results of the direct and splitting tensile strength are shown in the Figure 10 and Figure 11 below and all experimental results are given in Table 4.

The substitution of 30% of natural gravel or sand by RC aggregates does not affect significantly the evolution of the tensile strength whereas a substitution of 100% of natural aggregate induced a decrease of the tensile strength by 0.23 and 0.32 MPa at ages of 24 and 300 hours respectively. On hardened concrete, similar results were obtained by Sadati and Khayat [14] on recycled concrete composed of different type of recycled gravel and for half and full replacement of natural gravel by recycled one. Omary et al. [56] observed a stronger decrease of tensile strength due to the replacement of 30% of sand, but their tests were performed at 28 days.

330 Table 4. Results of the direct and splitting tensile strength

| **0RS-0RG** | | | | | | | | | | |
|---|---|---|---|---|---|---|---|---|---|---|
| **Age [h]** | 7 | 10 | 16 | 20 | 24 | | | | | |
| **ft,d [MPa]** | 0.03 | 0.06 | 0.29 | 0.52 | 0.71 | | | | | |
| **$\varepsilon_t$ [µm/m]** | 13.1 | 7.3 | 19.5 | 28.7 | 34.2 | | | | | |
| **Age [h]** | 17 | 21 | 24 | 25 | 36 | 48 | 73 | 108 | 168 | 300 |
| **0.9 x ft,sp [MPa]** | 0.47 | 0.64 | 0.71 | 0.88 | 1.05 | 1.20 | 1.40 | 1.60 | 1.66 | 1.77 |
| **0.75 x ft,sp [MPa]** | 0.39 | 0.53 | 0.59 | 0.74 | | | | | | |
| **30RS-0RG** | | | | | | | | | | |
| **Age [h]** | 7 | 10 | 16 | 20 | 24 | | | | | |
| **ft,d [MPa]** | 0.03 | 0.08 | 0.22 | 0.39 | 0.59 | | | | | |
| **$\varepsilon_t$ [µm/m]** | 13.3 | 11.6 | 18.3 | 25.7 | 34.1 | | | | | |
| **Age [h]** | 17 | 22 | 23 | 26 | 36 | 48 | 108 | 142 | 168 | 299 |
| **0.9 x ft,sp [MPa]** | 0.41 | 0.58 | 0.57 | 0.77 | 0.82 | 1.04 | 1.35 | 1.55 | 1.62 | 1.74 |
| **0.75 x ft,sp [MPa]** | 0.34 | 0.48 | 0.48 | 0.64 | | | | | | |
| **0RS-30RG** | | | | | | | | | | |
| **Age [h]** | 7 | 10 | 16 | 20 | 24 | | | | | |
| **ft,d [MPa]** | 0.03 | 0.07 | 0.27 | 0.42 | 0.65 | | | | | |
| **$\varepsilon_t$ [µm/m]** | 13.2 | 9.5 | 16.9 | 21.9 | 30.4 | | | | | |
| **Age [h]** | 18 | 22 | 24 | 26 | 36 | 47 | 141 | 168 | 299 | |
| **0.9 x ft,sp [MPa]** | 0.55 | 0.62 | 0.64 | 0.85 | 0.84 | 1.03 | 1.50 | 1.58 | 1.67 | |
| **0.75 x ft,sp [MPa]** | 0.46 | 0.52 | 0.53 | 0.71 | | | | | | |
| **0RS-100RG** | | | | | | | | | | |
| **Age [h]** | 7 | 10 | 16 | 20 | 24 | | | | | |
| **ft,d [MPa]** | 0.02 | 0.05 | 0.24 | 0.38 | 0.48 | | | | | |
| **$\varepsilon_t$ [µm/m]** | 14.5 | 9.8 | 19.8 | 26.2 | 29.0 | | | | | |
| **Age [h]** | 18 | 22 | 24 | 27 | 36 | 48 | 107 | 168 | 300 | |
| **0.9 x ft,sp [MPa]** | 0.44 | 0.63 | 0.48 | 0.79 | 0.68 | 0.85 | 1.10 | 1.34 | 1.45 | |
| **0.75 x ft,sp [MPa]** | 0.37 | 0.53 | 0.40 | 0.66 | | | | | | |

331

332

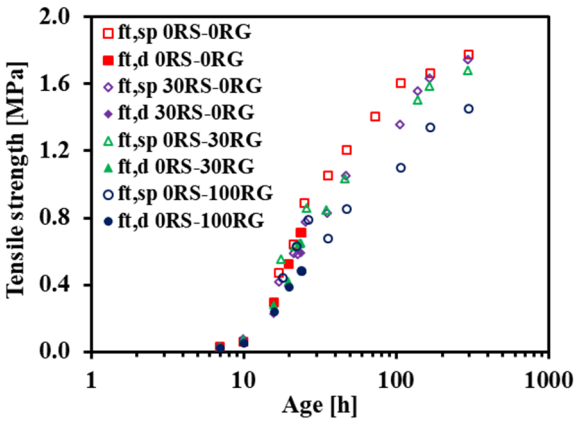


Figure 10. Effect of substitution rate on the tensile strength, determined from direct and splitting tensile tests

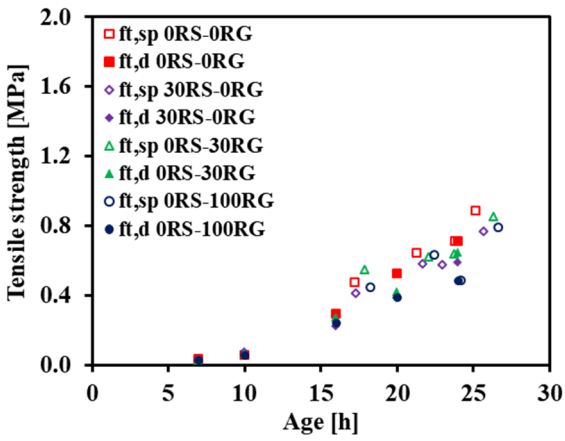


Figure 11. Zoom of the Figure 10 during the first 30 hours.

333

334 Between 16 and 24 hours, the tensile strength obtained by means of splitting and direct
335 tensile tests are not well superimposed. Higher values of the tensile strength are obtained
336 with the splitting tensile test. To improve the correlation between the direct and the
337 splitting tensile strength, the 0.9 factor from Equation 7 is replaced by a value of 0.75 for
338 all concrete mixtures at very early age (age lower than 30 hours). A good agreement is
339 then obtained between splitting and direct tensile tests as shown in the Figure 12 for very
340 early age results.

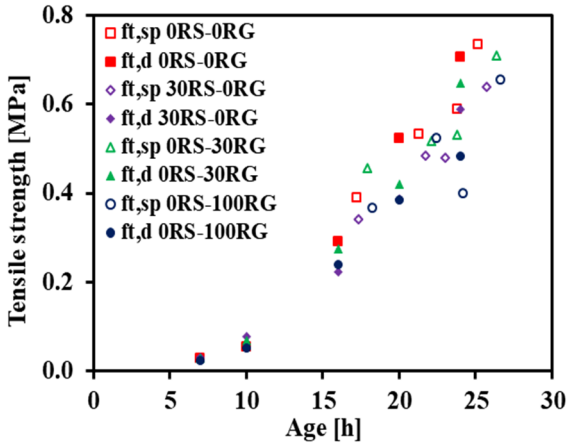


Figure 12. Tensile strength determined from direct and splitting tensile tests with correction

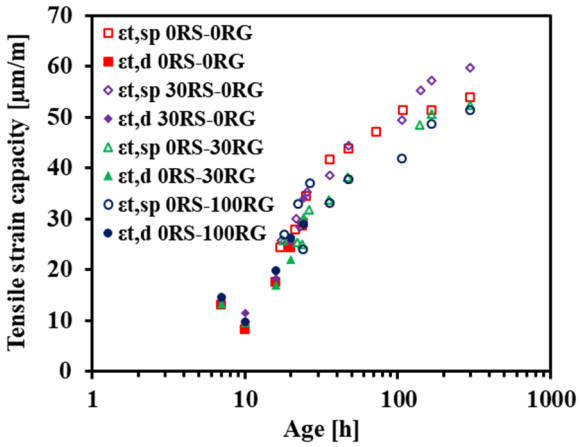


Figure 13. Effect of substitution rate on the tensile strain capacity: Determined from direct and splitting tensile tests

Based on the results of the tensile strength and the elastic modulus, the tensile strain capacity was defined according to Equation 8:

$$\varepsilon_t = \frac{f_t}{E} \quad \textbf{(8)}$$

Results of the tensile strain capacity of each material are plotted in Figure 13 according to the age of the material. Before setting, a decrease of the tensile strain capacity is observed for each concrete composition. A minimum is reached at an age of 10 hours with values close to 10 µm/m. Then the tensile strain capacity increases. At an age of 24 hours, the reference composition 0-RS-0RG reaches a tensile strain capacity of 34 µm/m. The substitution of 30% of natural sand by recycled one does not change significantly the evolution of the tensile strain capacity whereas a substitution of natural gravel by recycled ones induces a slight decrease of the tensile strain capacity by 5 µm/m at an age of 24 hours. Recycled gravel has lower elastic modulus thus concrete should show higher tensile strain capacity but concretes with recycled gravel also had lower tensile strength. Taking into account the repeatability of this characterization, there are few significant differences between studied materials. This is consistent with previous study of the authors [28] on the influence of aggregate type on tensile

properties. During the first 24 hours, the development of tensile strain capacity was mainly driven by the hydration of cement paste.

### 3.3 Restrained shrinkage and related properties

#### 3.3.1. Free strain

As the water-to-cement ratio of studied mixtures is relatively high, the autogenous deformations are relatively low and the main part of the shrinkage development is associated to the plastic shrinkage, i.e. the monitoring of strains in drying conditions at 20°C and 50% RH. Figure 14 gives the evolution of the free strain in the twin mold for concrete samples exposed to drying since casting. The development of the free strain can be divided in three stages. The first stage shows a rapid increase of the shrinkage with a magnitude of 20 to 30µm/m and takes place between the final setting and an age of around 20 hours. During this period, the development of the free strain is mainly driven by the self-desiccation of the cement paste [16]. The presence of recycled gravel and sand decreases slightly the shrinkage magnitude. This difference is more pronounced with recycled gravels. At an age of around 20 hours, the shrinkage rate decreases significantly for each composition. For composition with no or moderate amount of recycled aggregate, the second stage stops at an age of around 48 hours. For high replacement of natural gravels by recycled ones, the duration of the second stage takes place on a longer duration. It is also observed that the shrinkage rate is slightly lower during this stage for the concrete composed of recycled aggregate. After this period, the shrinkage rate increases again. No significant difference is observed during this third stage between the compositon without recycled aggregate and the compositions with moderate amount of recycled aggregate. The 100% RG concrete had the lowest shrinkage rate. The monitoring of free strains stopped when the concrete specimen of restrained shrinkage frame cracked, except for ORS-100RG concrete that did not crack.

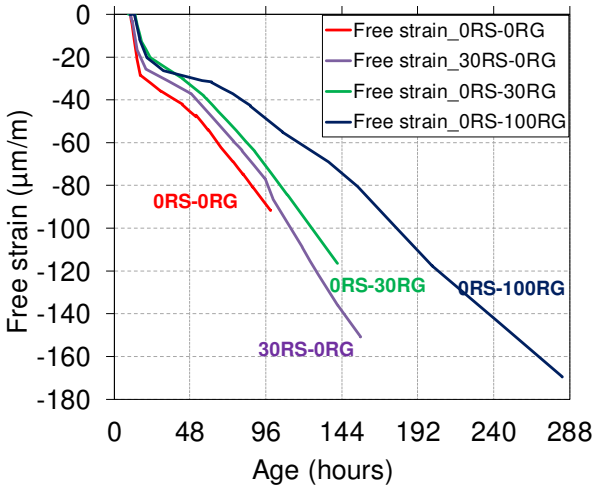


Figure 14. Free strain in twin mold.

The influence of internal curing on concretes with RG and RS can be observed from final setting to 48 hours on the evolution of the free strain, and then this effect remains significant only for 0RS-100RG concrete. The RG seems to mitigate self-desiccation and desiccation by maintaining the internal relative humidity at a higher level and lowering capillary pressures. Several aggregate properties influence the autogenous and drying shrinkage as the content and the porosity of the aggregate, the elastic modulus of the aggregate, the particle size distribution and the microstructure [20,59,60]. The magnitude of the internal curing of the recycled aggregate is function of the mean distance between two adjacent aggregates. The lower this distance, the higher the water released from the aggregates reaches the whole volume of cement paste [20]. This can explain why the internal curing effect provided by the recycled aggregates is much greater in the case of the composition 0RS-100RG than for the composition 0RS-30RG. These results are in agreement with previous study [25]. The autogenous shrinkage of concretes decreased as their replacement ratio increased, which was attributed to the higher water storage capacity of recycled concrete aggregates. On the other hand, the lower stiffness of the recycled gravel is a cause of higher shrinkage due to the lower restraint of the shrinkage of the cement paste [61] as observed by Maruyama and Sato [22] on high performance concretes composed of recycled gravels. In addition, recycled gravel

consists of natural gravels and hardened cement paste. Under the effect of drying, the latter shrinks. [62,63]. It therefore appears that the internal curing effect of recycled gravels is predominant on autogenous and drying shrinkage at a very early age for high replacement ratio of natural gravel by recycled ones.

When comparing the 30RS-00RG and 00RS-30RG concretes, it appears that, from an age of 96 hours, the shrinkage rate is higher for the 30RS-00RG composition. Both compositions have an equivalent amount of recycled aggregate, only the size of the recycled gravel and the content of old cement paste change. Recycled sand has high fine particle content (2% passing at 63µm and 7% at 125µm) and a higher content of old paste. Moreover, drying shrinkage is actually known to increase with paste volume [64,65]. Thus the use of recycled sand promotes in the same time the internal curing effect and the shrinkage of the recycled aggregate. It is therefore observed that the use of fine recycled aggregate increases the drying shrinkage in comparison to recycled gravels. Thus it is concluded from these results that the internal curing effect is significant for high replacement ratio of natural aggregates by recycled ones and that the use of fine recycled aggregate reduces the apparent internal curing effect of recycled aggregate due to their high shrinkage under drying conditions. The studies related to early-age shrinkage of concrete with recycled aggregates are relatively scarce. Hanif et al. [66] found that using recycled aggregates resulted in a lower net shrinkage strain.

### 3.3.2. Strain development under restrained condition

Cumulated strains under restrained conditions are plotted in Figure 15. From 24 hours their evolution significantly differs from free shrinkage (Figure 14). Under restrained conditions, a linear increase is observed for 0RS-0RG concrete and the concretes with RC aggregates show a decreasing rate, whereas the shrinkage rate is constant or increasing during this period under free conditions. The 30RS-0RG concrete even shows relative swelling from 24 to 48 hours.

Given the boundary conditions of TSTM and twin molds, this difference is due to creep strains. Subtracting the free strains (obtained from the twin mold) and the elastic strains from those in the TSTM mold provides the evolution of creep strain (Figure 16).

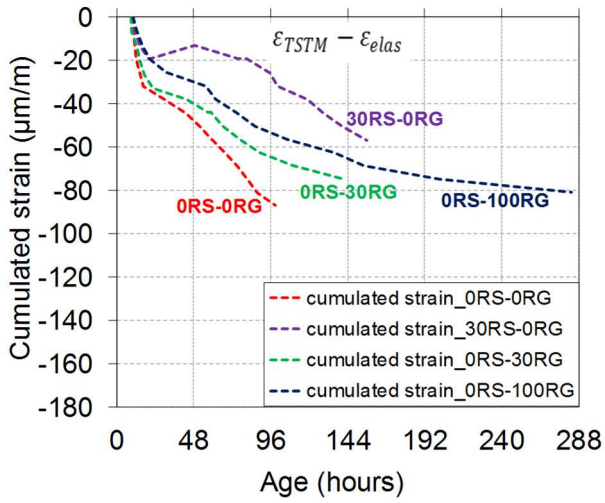


Figure 15. Effect of substitution rate on cumulated strain (TSTM mold)

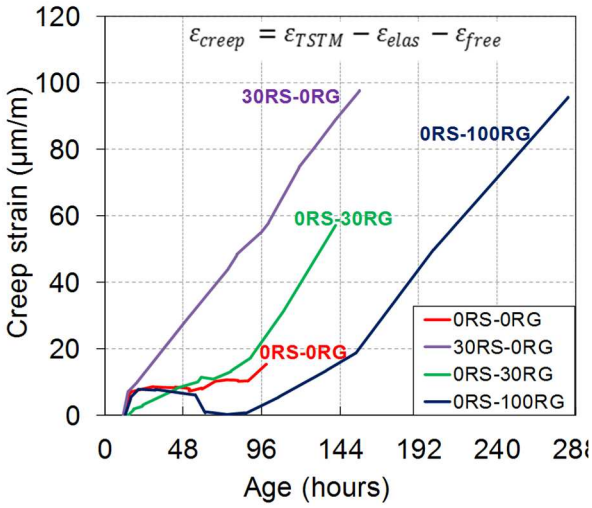


Figure 16. Evolution of creep strain calculated from free and restrained shrinkage evolutions

The reduction in shrinkage rate increases with RG content (Figure 15). This allowed delaying cracking time. 0RS-0RG and 0RS-30RG concrete cracked at strains of approximately 80 µm/m and 0RS-100RG reached this strain at 288 hours (12 days) without cracking. This value is of the order of magnitude of tensile strain capacity of concrete at early-age [5,28] but lower than the values of tensile strain capacity provided by direct tensile testing (Figure 13). Direct tensile test mainly characterizes the elastic behavior, with relatively low contribution of creep, whereas the contribution of creep during TSTM test is significant due to the duration of the test. As a consequence, if the tensile strain capacity is defined as the strain at cracking time, the TSTM test provides higher values than direct tensile test.

439 The lowest strain has been measured for the 30% RS concrete. However, this mixture has the
440 highest free strain at cracking. The creep of the 30% RS concrete actually started developing
441 just after 24 hours, while no creep could be detected for the other concretes. This concrete
442 mixture has not the highest proportion of RC aggregates but RS has a much higher content of
443 old paste than RG due to the crushing process [67]. The total content of old paste in 30RS-
444 0RG concrete is probably equal or higher than 0RS-100RG concrete. As early age creep is
445 mainly due to the formation and the behavior of CSH under loading and the water mobility
446 inside the cement paste [11,52], the observed evolution seems consistent with the composition
447 of studied concrete mixtures. From 96 hours the shrinkage rate of 30RS-0RG concrete was
448 approximately the same as 0RS-0RG concrete (Figure 14) and both concrete cracked. As
449 creep is related to the time-dependent behavior of concrete, the shrinkage rate is actually an
450 important parameter of shrinkage-induced cracking. If the stress development is too fast, it
451 cannot be mitigated by relaxation effects. Kovler and Bentur [68] actually took into account
452 the stress rate for the definition of an integrated criterion of cracking sensitivity. The creep
453 strains of 0RS-0RG concrete were relatively low but this concrete had relatively higher
454 shrinkage rate and the test stopped much earlier than the others (at 99 hours).

455 3.3.3. Stress development

456 The cracking sensitivity is assessed on the basis of the stress evolution and the tensile strength
457 (Figure 17). The 0RS-0RG concrete cracks first. Then the 0RS-30RG and 30RS-0RG
458 concrete crack. This concrete showed relative expansion around 48 hours (Figure 15), which
459 is consistent with the evolution of cumulated strains, then the stress increases again at higher
460 rate than 0RS-30RG. 0RS-100RG does not cracked and the cumulated stress is still much
461 lower than the tensile strength after 12 days.

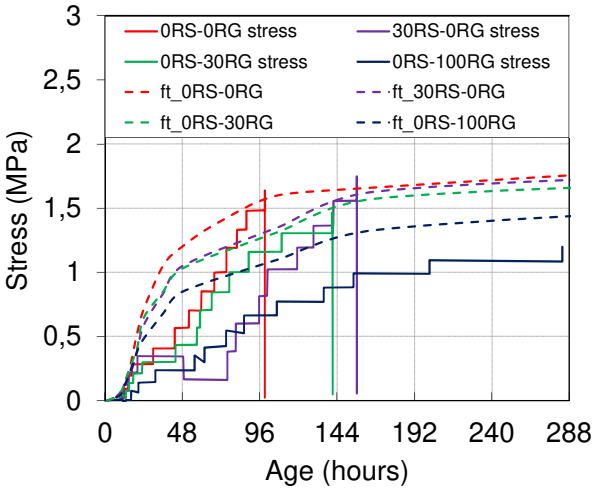


Figure 17**.** Tensile stresses from TSTM test and tensile strength.

Cracking is assumed to take place at the time corresponding to the intersection between the strength and stress curves [27,29]. Table 5 summarizes the data from the TSTM tests and direct tensile testing. From these results, the samples cracked when the stresses were higher or very close to the tensile strength. The stress-to-strength ratio at cracking was lower for the studied RC aggregate concrete mixtures, which suggests that their fracture energy was lower.

| Table 5**.** Properties of concrete at cracking time | **0RS-0RG** | **30RS-0RG** | **0RS-30RG** | **0RS-100RG** |
|---|---|---|---|---|
| Start of the test (h) | 10.2 | 10.2 | 9.3 | 10.2 |
| Age of cracking (h) | 99.1 | 156.2 | 141.1 | > 290* |
| Cracking stress (MPa) | 1.64 | 1.75 | 1.52 | / |
| Tensile strength at the age of cracking (MPa) | 1.42 | 1.65 | 1.51 | / |

*The test was stopped with no cracking.

The evolution of stresses cannot be fully understood without taking into account the elastic modulus of concrete. However there are coupled effects: the elastic modulus influences the stress development, but the stress is also likely to affect the development of elastic properties by creating damage or influencing the growth of hydration products. As 3 out of 4 concretes

cracked, high stress levels were actually reached. In order to estimate the coupling effects, two evolutions were assessed from experimental results, namely: static modulus in compression $E_{stat}$, and the modulus determined during TSTM compensation cycles $E_{TSTM}$, as detailed in sections 2.2.3 and 2.2.4 respectively. Figure 18 illustrates the results of the modulus provided by the TSTM test. These can be compared to the values provided by the repeated loadings in compression on cylindrical samples (

Figure 9) by plotting the $E_{TSTM}/E_{stat}$ ratio (Figure 19). This graph highlights the influence of damage in concrete during the restrained shrinkage test. It is interesting to note that an important reduction of $E_{TSTM}$ occurs only for high replacement of natural gravels by recycled ones whereas such reduction is also observed with recycled sand on $E_{stat.}$ In addition, it is observed for each composition that the time-evolutions and the maximal values of $E_{TSTM}$ were significantly different from $E_{stat}$. These differences of development between $E_{stat}$ and $E_{TSTM}$ can be related to many phenomena. $E_{stat}$ was measured in compression whereas $E_{TSTM}$ was measured in tension. According to the literature, the elastic modulus seems to be slightly higher in tension than in compression. This difference varied between 9 and 15% generally [69–73], which can be related to the difference of stress level and the influence of microcracking process [51]. It was also observed that the elastic modulus is influenced when shrinkage is restrained [74] or when a sustained load is applied [75]. In such conditions, a coupling between creep and damage exists [76,77] and results in a reduction of the elastic modulus. In this study the results plotted on Figure 19 show that $E_{TSTM}$ was lower than $E_{stat}$ from the beginning of the tests, although it was measured in tension. This suggests that the effects of loading under restrained conditions prevailed during the whole test.

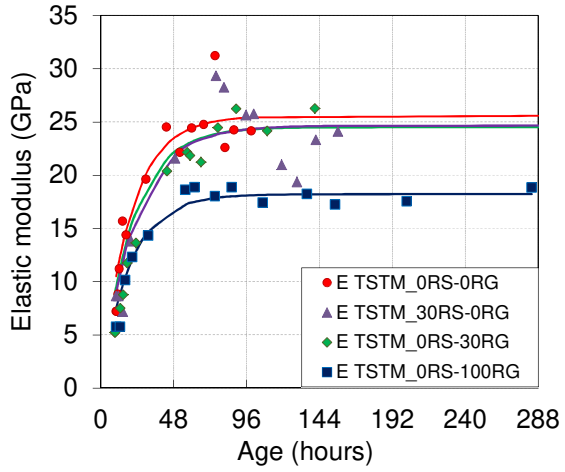


Figure 18. Effect of substitution rate on elastic modulus: Determined from TSTM tests

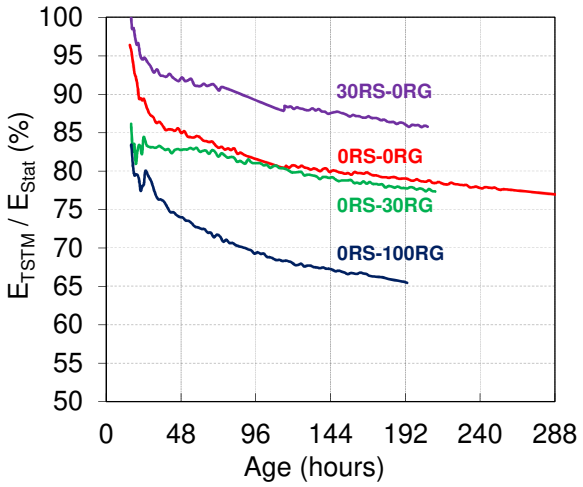


Figure 19. Ratio of elastic moduli measured under repeated loading $E_{Stat}$ and TSTM tests $E_{TSTM}$

499

500 The TSTM characterization of 0RS-0RG concrete stopped at 4 days due to cracking. The
501 values of the other concretes show a stabilization of $E_{TSTM}$ from 4 days. The shrinkage rate
502 (Figure 14) and stress rate (Figure 17) were actually high between 48 and 96 hours. Thus
503 relatively high loading levels were reached at this age. This could have generated damage
504 which could not be recovered by subsequent hydration. The $E_{stat}$ curves actually showed a
505 limited increase after 96 hours. The 0RS-0RG concrete showed the fastest increase of $E_{TSTM}$,
506 which could partly explain its high stress rate (Figure 17). The evolution of 0RS-30RG
507 properties was close. The most significant effect of damage was observed on 0RS-100 RG
508 concrete (Figure 19). The crushing process is likely to generate damage in RC aggregates and
509 concretes with RC aggregates have more ITZ [78]. From these points of view the evolution of
510 $E_{TSTM}$ of 30RS-0RG concrete is not obvious. During the first 72 hours it showed
511 approximately the same evolution as 0RS-30RG concrete (Figure 18). Both concrete mixtures
512 had approximately the same tensile strength but the stresses were much lower for 30RS-0RG

513 concrete between 48 and 96 hours thus lower loading rate allowed the development of elastic
514 modulus with less damage and coupled effects.

515

516 **3.4 Discussion on the influence of recycled concrete aggregates**

517 The discussion presented in this section is an attempt to quantify the contribution of the main
518 phenomena involved in shrinkage-induced cracking from the data gathered in previous
519 sections. The evolutions of shrinkage and elastic modulus can be used to deduce the effect of
520 relaxation and damage on the development of internal stress. Two stress evolutions are
521 actually needed. The first one is estimated during each TSTM test cycle from the $E_{TSTM}$
522 modulus and the free strain (measured on the twin mold at each cycle) according to equation
523 9. The difference between the calculated elastic stress and the measured stress gives the
524 relaxation. It depends on the evolution of the $E_{TSTM}$ modulus and the difference between free
525 and cumulated stresses.

$$\sigma(t_i) = \sum_{j=1}^{i} E_{TSTM}(t_j) \cdot \left(\varepsilon_{free\ sh.}(t_j) - \varepsilon_{free\ sh.}(t_{j-1})\right) \quad (9)$$

526 The second calculated stress uses the same equation (equation 9), but the $E_{TSTM}$ modulus is
527 replaced by the static modulus determined from repeated loading tests. From this difference
528 between both calculated elastic stresses, the effect of damage and couplings on the stress
529 development can be determined.

530 Both computed stress evolutions and experimental stress evolutions are presented in Figure
531 20. During the first hours after setting, the calculated stresses progress in a similar way to the
532 experimental stress. Then differences are observed and increased after each compensation
533 cycle. A divergence takes place before an age of 24 hours for the concretes 0RS0RG and
534 30RS0RG. During this period, the stress to strength ratio is close to 1 and a significant

535 influence of the creep/relaxation phenomenon is observed. For concretes composed of 30 and
536 100% of recycled gravel, this divergence occurs later at an age of 78 and 104 hours
537 respectively. The presence of recycled gravel delays the impact of the creep/relaxation
538 phenomenon during the first days after setting when concrete is under restrained conditions. A
539 divergence is also observed between both computed stresses and is associated to the
540 generation of damage when concrete shrinkage is restrained. The impact of damage is mainly
541 observed on concretes composed of recycled gravels and this effect is more pronounced for
542 the composition with higher recycled gravels content. On the other hand, the development of
543 the damage decreases for concrete composed of recycled sand.

544 As shown in Figure 20, the contribution of relaxation, damage and coupling effects
545 significantly decreases the magnitude of the stress development and, in consequence, delays
546 or cancels the cracking. The time when both computed stresses and the experimental stresses
547 exceed the tensile strength is also shown in Figure 20. It is observed that damage delays the
548 cracking of 5, 3, 20 and 51 hours whereas both damage and relaxation delay the cracking of
549 16, 67, 72 and more than 180 hours for the concrete 0RS0RG, 30RS0RG, 0RS30RG and
550 0RS100RG respectively.

551

552

553

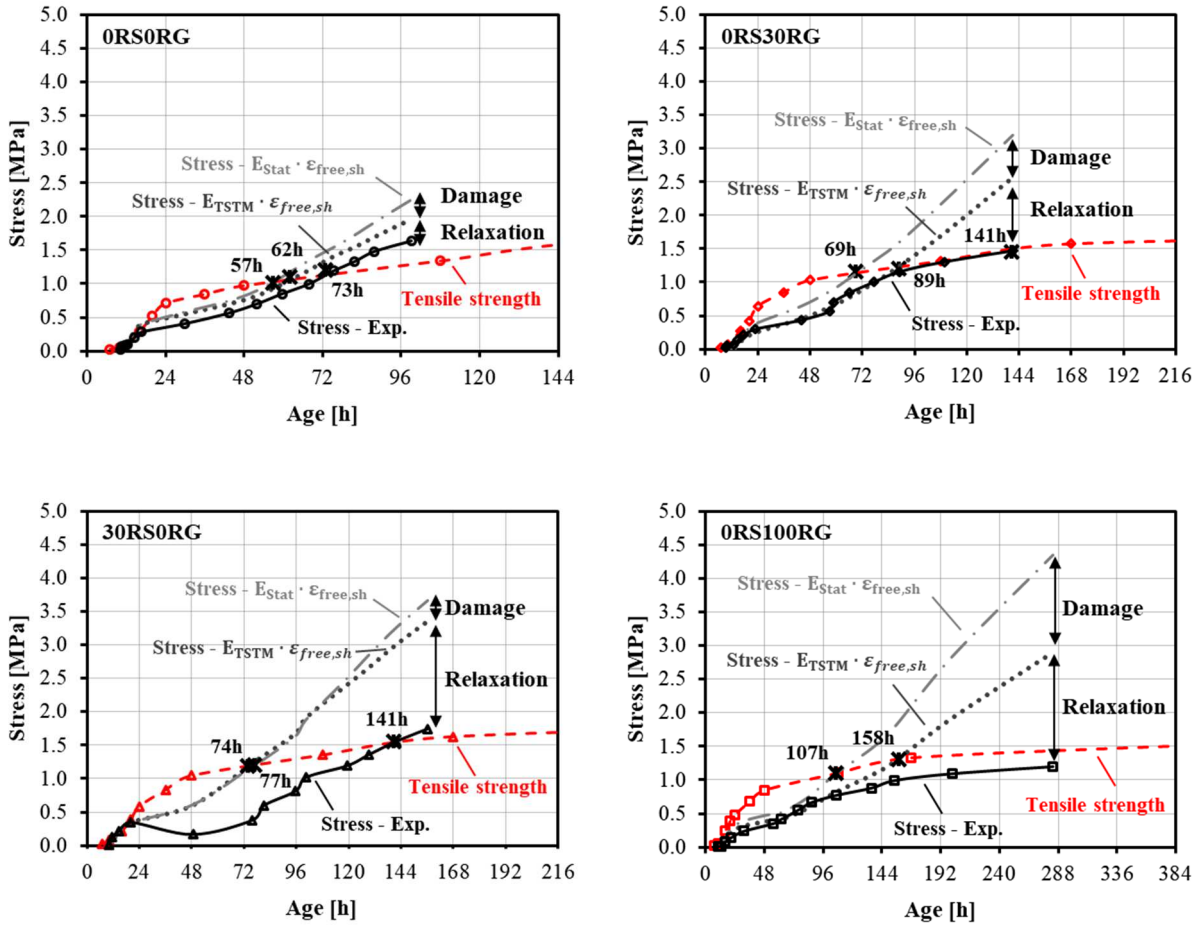


Figure 20. Evolution of experimental cumulated stress (Stress – Exp.), calculated elastic stress and tensile strength

554

555 The influence of recycled aggregate on the measured stresses, relaxation, damage, and
556 coupling effects is quantified in Figure 21. The values given in Figure 21 correspond to
557 cracking time or end of test if cracking does not occur. The analysis shows the significant
558 influence of these phenomena on the evolution of cracking sensitivity. Tensile strength
559 decreases with RC content (Figure 17), elastic stresses increase with RC content (maximum
560 values in Figure 21) whereas the experimental stresses decrease with RC content. Thus it is
561 shown that an elastic calculation would lead to the conclusion that the cracking sensitivity
562 increases with RC content, which is in reality not the case when considering creep/relaxation,
563 damage and couplings.

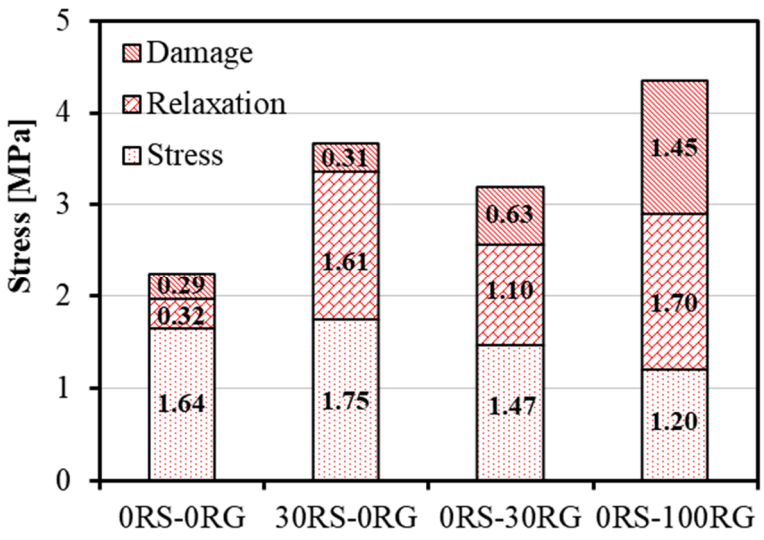


Figure 21. Experimental and calculated stresses at the end of TSTM tests.

These results confirm the prevailing influence of relaxation. This has already been showed in Figure 15 and Figure 16 through the difference between free and restrained deformations. Creep is beneficial to the behavior of concretes regarding cracking. It is also interesting to note the influence of relaxation on the final value of stress (Figure 21). It is shown that relaxation increases with RG content. Several experimental studies have been performed on the influence of RC aggregates on creep. Most of them showed that creep increases with RC content, even at relatively low contents. Domingo-Cabo et al. [8] actually reported that the specific creep of hardened RC concretes increased by 25, 29, and 32% for coarse RC aggregates proportions of 20, 50, and 100%. On hardening concrete, Delsaute, et al. [34] showed that the specific creep increases by 60% at very early age for concrete composed of recycled aggregate, whereas, at later ages, this increase is limited to 15-20% for concrete with recycled gravel and to 30% for concrete with recycled sand. Most of these studies deal with compressive creep whereas tensile creep occurs during restrained shrinkage tests. Klausen et al. [79] reported in a recent study that concrete had the same behavior in tension and compression, by using the same testing frame and procedure for both series of tests. One can

579 also note the influence of RC aggregates properties. 30RS-0RG and 0RS-100RG concrete
580 finally had the same stress decrease due to relaxation whereas the second concrete had higher
581 RC content. This can be attributed to the higher paste content of RS resulting from the
582 crushing process. This is consistent with $E_{stat}$ data (Figure 19), as both concretes had the same
583 values. Experimental studies on the same materials have shown that the finest particles (below
584 0.5 µm) have significant paste content [42].

585 The contribution of damage and coupling effects also increases with the proportion of RC
586 aggregates. This was even clearer for coarse RC aggregates (Figure 21). Zheng et al. [80] and
587 Grondin and Matallah [81] showed a significant influence of the ITZ thickness on the relative
588 Young's modulus of concrete and the properties of ITZ on the progress of damage in
589 concrete. Königsberger and Staquet [35] also showed through a numerical study that the ITZ
590 between old cement paste and aggregates triggers macroscopic failure.

591 30RS-0RG and 0RS-100RG concretes had approximately the same contribution of creep at
592 the end of TSTM test (Figure 21) but the influence of damage and coupling effects was
593 different. This has already been highlighted by the evolutions of elastic moduli (Figure 18 and
594 Figure 19). Both concretes actually had different stress histories during the first days and this
595 could have affected the development of mechanical properties (see section 3.2). They also had
596 different microstructures. The study of Guo et al. [82] concluded on weak bond between
597 coarse RC aggregates and new mortar but this cannot be extrapolated to the bond between RC
598 sand and new paste. RC sand has actually higher content of cement paste than RG, as
599 indicated by its higher absorption [83]. RS particles have lower elastic modulus, which results
600 in lower restraining effect for the shrinkage of cement paste inducing less cracks when
601 exposed to drying. The mechanical analysis performed by Le et al. [84] showed a good
602 bonding between RS particles and the new cement matrix at 28 days of hydration, which
603 might be attributed to a good chemical affinity between old and new pastes and to the surface

roughness of the RC aggregate. They used SEM and nano-indentation to investigate the properties of ITZ. A decrease of porosity was observed in the first ten micrometers for saturated sand, but the ITZ between saturated RS and cement paste is larger than with dried RS [63]. The same authors showed that the finest fractions of RS have the worst influence on mechanical properties. Finally, the elastic and creep deformations of 30RS-0RG were relatively high due to its high content of old paste but the damage or coupling effects were lower due to good bond between RS and new cement paste.

Consequently, the behavior of the concrete with 100% RG is interesting. The test has been performed during 12 days without appearance of cracking, although this type of concrete is known to have higher drying shrinkage magnitudes [8,85,86]. Regarding recycled concretes, the increase in shrinkage is associated with a decrease in modulus. Figure 21 gives the final value of stresses corresponding to different ages. However, at the age when 0RS-0RG concrete cracked, the 0RS-100RG concrete had much lower stresses and stress rate. This concrete had actually a lowest elastic modulus and the difference between the $E_{TSTM}$ values of both concretes was even higher (Figure 18 and Figure 19). At this time the benefit from internal curing was still significant thus shrinkage rate was also lower (Figure 14). Then shrinkage developed but concrete had gained some strength and creep mitigated the stress development. These results confirm that the cracking sensitivity is highly influenced by the evolution of shrinkage, elastic parameters and relaxation and each phenomenon had a significant influence of the development of stresses.

## 4. Conclusion

The present study focuses on the cracking sensitivity of recycled concrete under drying conditions at early age. The substitution of natural sand and gravel by recycled concrete aggregates is studied on four concretes for which recycled sand corresponds to 0 – 30% of the

sand volume fraction and recycled gravel corresponds to 0 – 30 – 100% of the gravel volume fraction. A Temperature-Stress Testing Machine (TSTM) was associated to other advanced techniques in order to investigate the main properties of recycled concrete under free and restrained conditions.

Under free conditions, the development of the elastic static modulus, tensile strength and free shrinkage have been experimentally defined, it is observed that:

- A reduction of the elastic modulus occurs when replacing natural aggregates by recycled ones. This reduction is more pronounced in presence of fine recycled aggregate for which the content of old cement paste is higher.
- Moderate content of recycled aggregate (<30%) does not affect significantly the development of the tensile strength whereas a full replacement of natural aggregate by recycled one decreases the tensile strength by 20%.
- The internal curing effect of recycled gravels delays and slows down the development of the free shrinkage at early age. This effect is more pronounced for high replacement ratio of natural gravels by recycled ones. The free shrinkage rate increases for concrete composed of recycled sand. This is induced by the high content of old cement paste which shrinks under drying condition.

Under restrained conditions, the development of the elastic modulus, strain and stress have been characterized, it is observed that:

- The development of elastic properties was found to depend on the loading history due to restrained shrinkage and the proportion and nature of recycled aggregates. An important reduction of the elastic modulus occurs for high replacement of natural gravels by recycled ones.

- A lower development of the strain is obtained under restrained condition. This is due to the creep phenomenon. This effect is more pronounced with concrete composed of recycled aggregates and occurs earlier with recycled sand.
- A slower development of the stress takes place for concretes composed of recycled aggregate. The age of cracking is then delayed significantly in presence of recycled aggregate. The full replacement of natural aggregates by recycled ones increases this effect.

The comparison of the concrete properties under free and restrained conditions allows quantifying the relative contributions of the main phenomena involved in shrinkage-induced cracking at early-age. It is based on the determination of elastic stress evolutions from free shrinkage data and elastic moduli provided by TSTM under sustained loading and cyclic testing. From the results of this analysis, cracking sensitivity decreased with recycled concrete content in spite of lower tensile strength, due to the major influence of relaxation, but also damage and coupling effects. The major stress reduction was attributed to relaxation but the phenomena contributed with different kinetics. The reduction of elastic modulus due to tensile loading appeared from the first 24 hours while creep seemed to develop later, as tensile stress to strength ratio became higher. Damage and coupling effects had a significant influence on stress development, especially with 100% coarse recycled concrete aggregates. This could be due to the influence of aggregates on the properties of the interfacial transition zone with new cement paste and within recycled concrete aggregates. The concrete with 30% recycled concrete sand had a different behavior with earlier creep development and lower damage, which can be attributed to higher old paste content and better bonding between recycled concrete sand and new cement paste.

From the experimental analyses performed in this study, it seems possible to design concrete mixtures with significant proportions of recycled concrete aggregates without affecting their

early-age cracking sensitivity. The results are related to good quality recycled concrete, initially saturated aggregates and standard drying conditions. Good curing is still recommended as concrete slabs might be exposed to more severe drying conditions in terms of wind speed or relative humidity.

## Acknowledgements

The authors would like to thank the *Projet national* (National Project, France) *RECYBETON* and the *Agence Nationale de la Recherche* (National Research Agency, France) within *ECOREB* project ("*EcoConstruction par le Recyclage du Béton"*, in French, "Sustainable construction though recycling concrete") for their financial support and fruitful discussions. The provision of materials and mix-design by French National Project *RECYBETON* is gratefully acknowledged. COST Action TU1404 is also acknowledged has for funding the short-term scientific mission of Ahmed Z. Bendimerad at ULB.

## References

[1] Irex, RECYBETON, (2018) 1. https://www.pnrecybeton.fr/ (accessed September 20, 2018).

[2] J. de Brito, N. Saikia, Concrete with Recycled Aggregates in International Codes, in: Recycl. Aggreg. Concr. Use Ind. Constr. Demolition Waste, 2013: pp. 379–429. doi:10.1007/978-1-4471-4540-0_7.

[3] Irex, ECOREB, (2019).

[4] R. Landgren, Water-Vapor Adsorption-Desorption Characteristics of Selected Lightweight Concrete Aggregates, in: Proc. Am. Soc. Test. Mater. Philadelphia, 1964: pp. 830–845.

[5] P. Bamford, Early-Age thermal crack control in concrete, 2007.

[6] R. Cortas, E. Rozière, S. Staquet, A. Hamami, A. Loukili, M.-P. Delplancke-Ogletree, Effect of the water saturation of aggregates on the shrinkage induced cracking risk of concrete at early age, Cem. Concr. Compos. 50 (2014) 1–9. doi:10.1016/j.cemconcomp.2014.02.006.

[7] T. Mostafa, S. Parviz, Drying shrinkage behavior of recycled aggregate concrete, Concr. Int. 18 (1996)

703 58–61.
704 [8] A. Katz, Properties of concrete made with recycled aggregate from partially hydrated old concrete, Cem.
705 Concr. Res. 33 (2003) 703–711. doi:10.1016/S0008-8846(02)01033-5.
706 [9] A. Domingo-Cabo, C. Lázaro, F. López-Gayarre, M.A. Serrano-López, P. Serna, J.O. Castaño-Tabares,
707 Creep and shrinkage of recycled aggregate concrete, Constr. Build. Mater. 23 (2009) 2545–2553.
708 doi:10.1016/j.conbuildmat.2009.02.018.
709 [10] S. Marinković, V. Radonjanin, M. Malešev, I. Ignjatović, Comparative environmental assessment of
710 natural and recycled aggregate concrete, Waste Manag. 30 (2010) 2255–2264.
711 doi:10.1016/j.wasman.2010.04.012.
712 [11] F. Benboudjema, J. Carette, B. Delsaute, T. Honorio de Faria, A. Knoppik, L. Lacarrière, A. Neiry de
713 Mendonça Lopes, P. Rossi, S. Staquet, Mechanical properties, in: E.M.R. Fairbairn, M. Azenha (Eds.),
714 Therm. Crack. Massive Concr. Struct. - State Art Rep. RILEM Tech. Comm. 254-CMS, 2019: pp. 69–
715 114. doi:10.1007/978-3-319-76617-1_4.
716 [12] J. Thomas, N.N. Thaickavil, P.M. Wilson, Strength and durability of concrete containing recycled
717 concrete aggregates, J. Build. Eng. 19 (2018) 349–365. doi:10.1016/j.jobe.2018.05.007.
718 [13] M. Velay-Lizancos, I. Martinez-Lage, P. Vazquez-Burgo, The effect of recycled aggregates on the
719 accuracy of the maturity method on vibrated and self-compacting concretes, Arch. Civ. Mech. Eng. 19
720 (2019) 311–321. doi:10.1016/j.acme.2018.11.004.
721 [14] S. Sadati, K.H. Khayat, Restrained shrinkage cracking of recycled aggregate concrete, Mater. Struct.
722 Constr. 50 (2017). doi:10.1617/s11527-017-1074-y.
723 [15] J. Henschen, A. Teramoto, D.A. Lange, Shrinkage and creep performance of recycled aggregate
724 concrete, RILEM Bookseries. 4 (2012) 1333–1340.
725 [16] B. Delsaute, S. Staquet, Impact of recycled sand and gravels in concrete on volume change, Constr.
726 Build. Mater. under rev (n.d.).
727 [17] A. Bentur, S.I. Igarashi, K. Kovler, Prevention of autogenous shrinkage in high-strength concrete by
728 internal curing using wet lightweight aggregates, Cem. Concr. Res. 31 (2001) 1587–1591.
729 doi:10.1016/S0008-8846(01)00608-1.
730 [18] Z. Liu, W. Hansen, Aggregate and slag cement effects on autogenous shrinkage in cementitious
731 materials, Constr. Build. Mater. 121 (2016) 429–436. doi:10.1016/j.conbuildmat.2016.06.012.
732 [19] S. Zhutovsky, K. Kovler, A. Bentur, Efficiency of lightweight aggregates for internal curing of high

733 strength concrete to eliminate autogenous shrinkage, Mater. Struct. Constr. 34 (2002) 97–101.
734 [20] R. Henkensiefken, D. Bentz, T. Nantung, J. Weiss, Volume change and cracking in internally cured
735 mixtures made with saturated lightweight aggregate under sealed and unsealed conditions, Cem. Concr.
736 Compos. 31 (2009) 427–437. doi:10.1016/j.cemconcomp.2009.04.003.
737 [21] S. Staquet, B. Delsaute, E.M.R. Fairbairn, R. Torrent, A. Knoppik, N. Ukrainczyk, E.A.B. Koenders,
738 Mixture proportioning for crack avoidance, 2019. doi:10.1007/978-3-319-76617-1_5.
739 [22] I. Maruyama, R. Sato, a Trial of Reducing Autogenous Shrinkage By Recycled Aggregate, Proc. Fourth
740 Int. Res. Semin. Rep. TVBM-3126, Gaithersburg, Maryland, USA. (2005) 264–270.
741 [23] G. Sant, M. Dehadrai, D. Bentz, P. Lura, C.F. Ferraris, J.W. Bullard, J. Weiss, Detecting the fluid-to-
742 solid transition in cement pastes, Concr. Int. 31 (2009) 53–58.
743 [24] M. Salgues, J.C. Souche, P. Devillers, E. Garcia-Diaz, Influence of initial saturation degree of recycled
744 aggregates on fresh cement paste characteristics: consequences on recycled concrete properties, Eur. J.
745 Environ. Civ. Eng. 22 (2018) 1146–1160. doi:10.1080/19648189.2016.1245630.
746 [25] A. Gonzalez-Corominas, M. Etxeberria, Effects of using recycled concrete aggregates on the shrinkage
747 of high performance concrete, Constr. Build. Mater. 115 (2016) 32–41.
748 doi:10.1016/j.conbuildmat.2016.04.031.
749 [26] J.C. Souche, A.Z. Bendimerad, E. Roziere, M. Salgues, P. Devillers, E. Garcia-Diaz, A. Loukili, Early
750 age behaviour of recycled concrete aggregates under normal and severe drying conditions, J. Build. Eng.
751 13 (2017) 244–253. doi:10.1016/j.jobe.2017.08.007.
752 [27] T.A. Hammer, K.T. Fosså, Ø. Bjøntegaard, Cracking tendency of HSC: Tensile strength and self
753 generated stress in the period of setting and early hardening, Mater. Struct. 40 (2007) 319–324.
754 doi:10.1617/s11527-006-9109-9.
755 [28] E. Roziere, R. Cortas, A. Loukili, Tensile behaviour of early age concrete: New methods of
756 investigation, Cem. Concr. Compos. 55 (2015) 153–161. doi:10.1016/j.cemconcomp.2014.07.024.
757 [29] D. Ravina, R. Shalon, Plastic Shrinkage Cracking, ACI J. Proc. 65 (1968) 282–292. doi:10.14359/7473.
758 [30] K. Kovler, Testing system for determining the mechanical behaviour of early age concrete under
759 restrained and free uniaxial shrinkage, Mater. Struct. 27 (1994) 324–330. doi:10.1007/BF02473424.
760 [31] O. Bjontegaard, Thermal dilation and autogenous deformation as driving forces to self-induced stresses
761 in high-performance concrete, 1999.
762 [32] T. Aly, J.G. Sanjayan, Shrinkage-cracking behavior of OPC-fiber concrete at early-age, Mater. Struct.

763 Constr. 43 (2010) 755–764. doi:10.1617/s11527-009-9526-7.
764 [33] T. Grazia, Comportement des bétons au jeune âge, PhD thesis, Université Laval, 1999.
765 [34] B. Delsaute, S. Staquet, Development of Strain-Induced Stresses in Early Age Concrete Composed of
766 Recycled Gravel or Sand, J. Adv. Concr. Technol. 17 (2019) 319–334. doi:10.3151/jact.17.319.
767 [35] M. Königsberger, S. Staquet, Micromechanical Multiscale Modeling of ITZ-Driven Failure of Recycled
768 Concrete: Effects of Composition and Maturity on the Material Strength, Appl. Sci. 8 (2018) 976.
769 doi:10.3390/app8060976.
770 [36] M.P. Adams, T. Fu, A.G. Cabrera, M. Morales, J.H. Ideker, O.B. Isgor, Cracking susceptibility of
771 concrete made with coarse recycled concrete aggregates, Constr. Build. Mater. 102 (2016) 802–810.
772 doi:10.1016/j.conbuildmat.2015.11.022.
773 [37] A. Darquennes, S. Staquet, M.-P. Delplancke-Ogletree, B. Espion, Effect of autogenous deformation on
774 the cracking risk of slag cement concretes, Cem. Concr. Compos. 33 (2011) 368–379.
775 doi:10.1016/j.cemconcomp.2010.12.003.
776 [38] S. Staquet, B. Delsaute, A. Darquennes, B. Espion, Design of a Revisited Tstm System for Testing
777 Concrete Since Setting Time Under Free and Restraint Conditions ., in: Concrack 3 - RILEM-JCI Int.
778 Work. Crack Control Mass Concr. Relat. Issues Concern. Early-Age Concr. Struct., 2012: p. 12.
779 [39] P. Gonçalves, J. De Brito, Recycled aggregate concrete (RAC) - Comparative analysis of existing
780 specifications, Mag. Concr. Res. 62 (2010) 339–346. doi:10.1680/macr.2008.62.5.339.
781 [40] K.P. Verian, W. Ashraf, Y. Cao, Properties of recycled concrete aggregate and their influence in new
782 concrete production, Resour. Conserv. Recycl. 133 (2018) 30–49. doi:10.1016/j.resconrec.2018.02.005.
783 [41] M. Arezoumandi, A. Smith, J.S. Volz, K.H. Khayat, An experimental study on flexural strength of
784 reinforced concrete beams with 100% recycled concrete aggregate, Eng. Struct. 88 (2015) 154–162.
785 doi:10.1016/j.engstruct.2015.01.043.
786 [42] T. Le, S. Rémond, G. Le Saout, E. Garcia-Diaz, Fresh behavior of mortar based on recycled sand -
787 Influence of moisture condition, Constr. Build. Mater. 106 (2016) 35–42.
788 doi:10.1016/j.conbuildmat.2015.12.071.
789 [43] NF EN 206/CN, Béton – Spécification, performance, production et confirmité – Complément national à
790 la norme NF EN 206, 2014.
791 [44] A.Z. Bendimerad, E. Rozière, A. Loukili, Plastic shrinkage and cracking risk of recycled aggregates
792 concrete, Constr. Build. Mater. 121 (2016) 733–745. doi:10.1016/j.conbuildmat.2016.06.056.

[45] A.Z. Bendimerad, E. Roziere, A. Loukili, Combined experimental methods to assess absorption rate of natural and recycled aggregates, Mater. Struct. 48 (2015) 3557–3569. doi:10.1617/s11527-014-0421-5.

[46] F. De Larrard, T. Sedran, Mixture-proportioning of high-performance concrete, Cem. Concr. Res. 32 (2002) 1699–1704. doi:10.1016/S0008-8846(02)00861-X.

[47] T. Sedran, Mise au point des formules de béton de référence, PN RECYBETON., (2013) 37.

[48] C. Boulay, S. Staquet, B. Delsaute, J. Carette, M. Crespini, O. Yazoghli-Marzouk, É. Merliot, S. Ramanich, How to monitor the modulus of elasticity of concrete, automatically since the earliest age?, Mater. Struct. 47 (2014) 141–155. doi:10.1617/s11527-013-0051-3.

[49] B. Delsaute, C. Boulay, J. Granja, J. Carette, M. Azenha, C. Dumoulin, G. Karaiskos, A. Deraemaeker, S. Staquet, Testing Concrete E-modulus at Very Early Ages Through Several Techniques: An Inter-laboratory Comparison, Strain. 52 (2016) 91–109. doi:10.1111/str.12172.

[50] M. Irfan-ul-Hassan, B. Pichler, R. Reihsner, C. Hellmich, Elastic and creep properties of young cement paste, as determined from hourly repeated minute-long quasi-static tests, Cem. Concr. Res. 82 (2016) 36–49. doi:10.1016/j.cemconres.2015.11.007.

[51] B. Delsaute, New approach for Monitoring and Modelling of the Creep and Shrinkage behaviour of Cement Pastes , Mortars and Concretes since Setting Time, Université Libre de Bruxelles (BATir) and Université Paris Est (IFSTTAR), 2016.

[52] B. Delsaute, C. Boulay, S. Staquet, Creep testing of concrete since setting time by means of permanent and repeated minute-long loadings, Cem. Concr. Compos. 73 (2016) 75–88. doi:10.1016/j.cemconcomp.2016.07.005.

[53] B. Delsaute, J.-M. Torrenti, S. Staquet, Modeling basic creep of concrete since setting time, Cem. Concr. Compos. 83 (2017) 239–250. doi:10.1016/j.cemconcomp.2017.07.023.

[54] A. Darquennes, Comportement au jeune âge de bétons formulés à base de ciment au laitier de haut fourneau en condition de déformations libre et restreinte, PhD thesis, Université Libre de Bruxelles, 2009.

[55] A.B.E. Klausen, Early age crack assessment of concrete structures: experimental investigation of decisive parameters, NTNU, 2016.

[56] S. Omary, E. Ghorbel, G. Wardeh, Relationships between recycled concrete aggregates characteristics and recycled aggregates concretes properties, Constr. Build. Mater. 108 (2016) 163–174. doi:10.1016/j.conbuildmat.2016.01.042.

[57] A.F. Stock, D.J. Hannant, R.I.T. Williams, The Effect of Aggregate Concentration Upon The Strength And Modulus Of Elasticity Of Concrete, Mag. Concr. Res. 31 (1979) 225–234. doi:10.1680/macr.1979.31.109.225.

[58] M. Velay-Lizancos, I. Martinez-Lage, M. Azenha, J. Granja, P. Vazquez-Burgo, Concrete with fine and coarse recycled aggregates: E-modulus evolution, compressive strength and non-destructive testing at early ages, Constr. Build. Mater. 193 (2018) 323–331. doi:10.1016/j.conbuildmat.2018.10.209.

[59] W.H. Kwan, M. Ramli, K.J. Kam, M.Z. Sulieman, Influence of the amount of recycled coarse aggregate in concrete design and durability properties, Constr. Build. Mater. 26 (2012) 565–573. doi:10.1016/j.conbuildmat.2011.06.059.

[60] N. Fonseca, J. De Brito, L. Evangelista, The influence of curing conditions on the mechanical performance of concrete made with recycled concrete waste, Cem. Concr. Compos. 33 (2011) 637–643. doi:10.1016/j.cemconcomp.2011.04.002.

[61] W. Hansen, J.A. Almudaiheem, Ultimate Drying Shrinkage of Concrete - Influence of Major Parameters., ACI Mater. J. 84 (1987) 217–223. doi:10.14359/1954.

[62] R. Le Roy, Déformations instantanées et différées des bétons à hautes performances, PhD thesis, Ecole Nationale des Ponts et Chaussées, Paris, France, 1995.

[63] T. Fujiwara, Effect of Aggregate on Drying Shrinkage of Concrete, J. Adv. Concr. Technol. 6 (2008) 31–44.

[64] B. Bissonnette, P. Pierre, M. Pigeon, Influence of key parameters on drying shrinkage of cementitious materials, Cem. Concr. Res. 29 (1999) 1655–1662. doi:10.1016/S0008-8846(99)00156-8.

[65] E. Rozière, S. Granger, P. Turcry, A. Loukili, Influence of paste volume on shrinkage cracking and fracture properties of self-compacting concrete, Cem. Concr. Compos. 29 (2007) 626–636. doi:10.1016/j.cemconcomp.2007.03.010.

[66] A. Hanif, Y. Kim, Z. Lu, C. Park, Early-age behavior of recycled aggregate concrete under steam curing regime, J. Clean. Prod. 152 (2017) 103–114. doi:10.1016/j.jclepro.2017.03.107.

[67] Z. Zhao, S. Remond, D. Damidot, W. Xu, Influence of fine recycled concrete aggregates on the properties of mortars, Constr. Build. Mater. 81 (2015) 179–186. doi:10.1016/j.conbuildmat.2015.02.037.

[68] K. Kovler, A. Bentur, Cracking sensitivity of normal- and high-strength concrete, 2009.

[69] I. Yoshitake, F. Rajabipour, Y. Mimura, A. Scanlon, A Prediction Method of Tensile Young's Modulus of Concrete at Early Age, Adv. Civ. Eng. 2012 (2012) 1–10. doi:10.1155/2012/391214.

[70] D.S. Atrushi, Tensile and Compressive Creep of Early Age Concrete : Testing and Modelling, PhD thesis, The Norwegian University of Sciences and Technology, Trondheim,Norway, 2003.

[71] B. Bissonnette, M. Pigeon, A.M. Vaysburd, Tensile creep of concrete: Study of its sensitivity to basic parameters, ACI Mater. J. 104 (2007) 360–368.

[72] S. Hagihara, S. Nakamura, Y. Masuda, M. Kono, Experimental study on mechanical properties and creep behavior of high-strength concrete in early age, Concr. Res. Technol. 11 (2000) 39–50.

[73] V.Y.G. Yanni, Multi-scale Investigation of Tensile Creep of Ultra High Performance Concrete for Bridge Applications, PhD thesis, Georgia Institute of Technology, 2009.

[74] J. Pacheco, J. De Brito, J. Ferreira, D. Soares, Flexural load tests of full-scale recycled aggregates concrete structures, Constr. Build. Mater. 101 (2015) 65–71. doi:10.1016/j.conbuildmat.2015.10.023.

[75] H.R. Sobuz, E. Ahmed, N.M. Sutan, N.M. Sadiqul Hasan, M.A. Uddin, M. Jahir Uddin, Bending and time-dependent responses of RC beams strengthened with bonded carbon fiber composite laminates, Constr. Build. Mater. 29 (2012) 597–611. doi:10.1016/j.conbuildmat.2011.11.006.

[76] P. Rossi, J.L. Tailhan, F. Le Maou, Creep strain versus residual strain of a concrete loaded under various levels of compressive stress, Cem. Concr. Res. 51 (2013) 32–37. doi:10.1016/j.cemconres.2013.04.005.

[77] M. Omar, A. Loukili, G. Pijaudier-cabot, Y. Le Pape, Creep-damage coupled effects: experimental investigation on bending beams with various sizes, J. Mater. Civ. Eng. 21 (2009) 65–72.

[78] G. Mazzucco, G. Xotta, B. Pomaro, V.A. Salomoni, F. Faleschini, Elastoplastic-damaged meso-scale modelling of concrete with recycled aggregates, Compos. Part B Eng. 140 (2018) 145–156. doi:10.1016/j.compositesb.2017.12.018.

[79] A.E. Klausen, T. Kanstad, Ø. Bjøntegaard, E. Sellevold, Comparison of tensile and compressive creep of fly ash concretes in the hardening phase, Cem. Concr. Res. 95 (2017) 188–194. doi:10.1016/j.cemconres.2017.02.018.

[80] J. Zheng, X. Zhou, X. Jin, An n-layered spherical inclusion model for predicting the elastic moduli of concrete with inhomogeneous ITZ, Cem. Concr. Compos. 34 (2012) 716–723. doi:10.1016/j.cemconcomp.2012.01.011.

[81] F. Grondin, M. Matallah, How to consider the Interfacial Transition Zones in the finite element modelling of concrete?, Cem. Concr. Res. 58 (2014) 67–75. doi:10.1016/j.cemconres.2014.01.009.

[82] M. Guo, S.Y. Alam, A.Z. Bendimerad, F. Grondin, E. Rozière, A. Loukili, Fracture process zone characteristics and identification of the micro-fracture phases in recycled concrete, Eng. Fract. Mech.

181 (2017) 101–115. doi:10.1016/j.engfracmech.2017.07.004.

[83] P. Belin, G. Habert, M. Thiery, N. Roussel, Cement paste content and water absorption of recycled concrete coarse aggregates, Mater. Struct. Constr. 47 (2014) 1451–1465. doi:10.1617/s11527-013-0128-z.

[84] T. Le, G. Le Saout, E. Garcia-Diaz, D. Betrancourt, S. Rémond, Hardened behavior of mortar based on recycled aggregate: Influence of saturation state at macro- and microscopic scales, Constr. Build. Mater. 141 (2017) 479–490. doi:10.1016/j.conbuildmat.2017.02.035.

[85] T.C. Hansen, E. Boegh, Elasticity and Drying Shrinkage of Recycled Aggregate Concrete, ACI J. 82 (1985) 648–652.

[86] T.C. Hansen, Recycled aggregates and recycled aggregate concrete: third state-of- the-art report 1945-1989, Recycl. Demolished Concr. Mason. (1992) 336.